Viral and immune dynamics of HPV genital infections in young women

Nicolas Tessandier[1,+], Baptiste Elie[2,+], Vanina Boué[2], Christian Selinger[2,3], Massilva Rahmoun[2], Claire Bernat[2,4], Sophie Grasset[2], Soraya Groc[2,5], Anne-Sophie Bedin[5], Thomas Beneteau[2], Marine Bonneau[6], Christelle Graf[6], Nathalie Jacobs[7], Tsukushi Kamiya[1], Marion Kerioui[8], Julie Lajoie[9], Imène Melki[1], Jean-Luc Prétet[10,11], Bastien Reyné[2], Géraldine Schlecht-Louf[12], Mircea T. Sofonea[5,13], Olivier Supplisson[1,14], Vincent Foulongne[5], Jérémie Guedj[8], Christophe Hirtz[16], Marie-Christine Picot[17], Jacques Reynes[18], Vincent Tribout[19], Édouard Tuaillon[5], Tim Waterboer[20], Michel Segondy[5], Ignacio G Bravo[2], Nathalie Boulle[5], Carmen Lia Murall[2,21], Samuel Alizon[1,2,*]

[1] CIRB, CNRS, INSERM, Collège de France, Université PSL, Paris, France
[2] MIVEGEC, CNRS, IRD, Université de Montpellier, France
[3] Swiss Tropical and Public Health Institute, Basel, Switzerland
[4] CNRS UMR 5203, Institut de Génomique Fonctionnelle, Montpellier, France
[5] Pathogenesis and Control of Chronic Infections, INSERM, CHU, University of Montpellier, Montpellier, France
[6] Department of Obstetrics and Gynaecology, Centre Hospitalier Universitaire de Montpellier, Montpellier, France
[7] Laboratory of Cellular and Molecular Immunology, GIGA Research, University of Liège, 4000 Liège, Belgium
[8] INSERM, IAME, Université de Paris, Paris, France
[9] Department of Medical Microbiology, University of Manitoba, Winnipeg, Manitoba, Canada
[10] EA3181, UBFC, LabEx LipSTIC ANR-11-LABX-0021, Besançon, France
[11] Centre National de Référence Papillomavirus, CHRU de Besançon, Besançon, France
[12] UMR996, Inflammation, Chemokines and Immunopathology, INSERM, Université Paris-Sud, Université Paris-Saclay, Clamart, France
[13] CHU de Nîmes, Nîmes, France
[14] Sorbonne Université, France
[16] RMB-PPC, INM, Univ Montpellier, CHU Montpellier, INSERM CNRS, Montpellier, France
[17] Department of Medical Information (DIM), Centre Hospitalier Universitaire de Montpellier, Montpellier, France

[18] Department of Infectious and Tropical Diseases, Centre Hospitalier Universitaire de Montpellier, Montpellier, France
[19] Center for Free Information, Screening and Diagnosis (CeGIDD), Centre Hospitalier Universitaire de Montpellier, Montpellier, France
[20] German Cancer Research Center (DKFZ), Infections and Cancer Epidemiology, Heidelberg, Germany
[21] National Microbiology Laboratory (NML), Public Health Agency of Canada (PHAC), Canada

[+] equal contribution
[*] Corresponding author: samuel.alizon@cnrs.fr

Human papillomavirus (HPV) infections drive one in twenty new cancer cases. Despite the potential for improving treatment, screening, and vaccination strategies, little is known as to why the vast majority of HPV infections clear spontaneously within two years. To untangle the dynamics of these non-persisting infections, we performed a combined quantitative analysis of virological, immunological, and clinical data from an original longitudinal cohort of 189 women with high temporal resolution. We find that HPV viral load reaches a plateau within two months, and clears within a median time of 14 months. Furthermore, we identify immune correlates associated with infection clearance, especially TCR-gamma-delta cells. Our results open new perspectives for understanding the frontier between acute and chronic infections and for controlling HPV-associated diseases.

Human papillomaviruses (HPVs) cause nearly all cervical cancers, the majority of many anogenital cancers, and a significant fraction of oropharyngeal cancers (*1*). Women and low-medium income countries are the most affected, with respectively 90% and 65% of the 630,000 HPV-induced cancers reported in 2012 worldwide (*1*). This burden, further exacerbated by millions of cases of anogenital warts (*2*), stems from the fact that HPVs are among the most prevalent sexually-transmitted infections (STIs), with a high transmission risk per sexual contact (*3*). Fortunately, more than 90% of these infections do not persist for more than two years in young adults (*4*–*7*). The factors driving infection clearance are poorly known and could involve the adaptive and the innate immune response (*8*), but also random events occurring during cell division (*9*, *10*). Over the last two decades, safe and efficient vaccines have been developed that target the most oncogenic genotypes (especially HPV16 and HPV18), as well as genotypes causing genital warts (HPV6 and HPV11) (*11*, *12*). Notwithstanding, chronic infections by HPVs will remain a major public health issue for at least one generation because of low vaccine coverage in many countries and decreased vaccine efficacy if administered after exposition (*13*). Non-persisting, or 'acute', HPV infections are often asymptomatic and benign but raise important challenges (*14*). First, the quality of screening policies relies on the description of the natural history of the infection (*15*). Furthermore, understanding interactions between HPVs and the immune system may shed new light on the factors that lead to clearance or chronicity, with implications for human cancers of infectious origin (*16*), and the development of immunotherapies (*17*). Finally, acute HPV infections represent a major reservoir of virus diversity, which could fuel an evolutionary response to vaccine-driven selective pressures (*18*). Unfortunately, although we have known for decades about the prevalence and duration of acute HPV infections (*4*, *5*, *19*), we still know little about the immune response they might elicit and temporal variations in virus loads.

To address this matter, we implemented a longitudinal cohort study in Montpellier (France) dur-

ing which 189 women aged from 18 to 25 years old were followed every two months until HPV infection clearance or for a maximum duration of 24 months (*20*). At each of the 974 on-site visits, biological samples were collected and participants filled in detailed socio-demographic, health, and behaviour questionnaires. The strength of the study stems from its temporal resolution and the quality of the biological data generated. The main characteristics of the cohorts are shown in Table S1 and in (*21*).

Immune response to HPV infections

HPV infections are poorly immunogenic and only 40 to 60% of HPV-positive women seroconvert to an incident viral genotype (*22*). Therefore, we focused on the local cellular immune response and used flow cytometry (FCM) to analyse cervical smears. These biological samples are particularly fragile and challenging to study because keratinocytes are highly adhesive and autofluorescent cells. Building on an existing protocol (*23*) and on existing software packages (*24*), we devised a pipeline to identify clusters of immune cell populations with a non-supervised approach. We first used this pipeline to identify leukocytes ($CD45^+$ cells). We then applied it on this cell population to automatically delineate 20 cellular clusters, which we could manually group into 11 distinct immune cell populations based on morphological and lineage markers (Fig. S2, S3, and Table S3). The most frequent cells were $CD16^+$ granulocytes (59.9%). We could also notably identify three distinct populations of TCR$\gamma\delta$ cells (clusters III, VII and IX), representing respectively 3.88%, 12.44%, and 0.73% of the $CD45^+$ cells (Fig S2), as well as CD4 and CD8 T cells (respectively 1.15% and 0.78%). Other cell populations could not be assigned formally but display features of local antigen-presenting cells (cluster V) or NK cells (cluster II) (Fig. S2).

We stratified the samples as HPV negative or positive for a 'focal' HPV genotype, *i.e.* a genotype detected at least during two consecutive visits (Fig. S1 and Table S2). This emphasis was

made to avoid a spurious focus on 'singletons', *i.e.* an HPV genotype detected at a single visit. These are sometimes referred to as 'transient infections' (*25*) and are a poor marker of actual infections (*26*). A UMAP clustering helped visualise the 11 immune cell populations and the composition shift in samples with a focal HPV, especially an increase of cluster VII (Fig. 1A). A differential abundance analysis (Fig. 1B) confirmed that focal HPV-positive samples exhibited a lower proportion of cluster X ($CD4^+$ T-cells) than HPV-negative samples (Fold Change, FC: 0.62) and a higher abundance of cluster VII ($CD45^{low}$ TCRγδ cells) and cluster VIII (FC: 1.71 and 1.41, Fig. 1B and C). Clusters IV, V, and VI were also rarer in focal HPV-positive samples (FC: 0.63, 0.71, and 0.67). These differences were statistically significant in a multivariate generalized linear mixed model including anti-HPV vaccination status as a fixed effect and a random effect accounting for the multiple sampling per participant (Fig. 1C). Differential expression analysis highlighted moderate changes for activation markers CD69 or CD161 fluorescence levels. We did find a reduced median signal intensity for CD69 on CD4 T cells, which suggests lower priming of CD4 T cells during focal HPV infections (cluster X, Fold change = 0.90, p-adj = 0.04) (Table. S4).

Building on previous results showing an association with HPV infections (*27*), we quantified the concentrations of five cytokines in cervical secretions using Meso Scale Discovery technology and normalised the values over total protein concentration. Associations with HPV status (Fig. S4) were consistent with earlier cross-sectional studies (*27*, *28*). To improve the characterization of immune cells, we explored correlations between the proportion of each immune cell population in a sample and the concentration of each cytokine in the same sample (Fig. 2A). Our linear models identified positive correlations between the concentration of IFNγ and the frequency of CD8 T cells (cluster XI, $\beta = 0.14$), although with a p-value of 0.062, and to a lower extent with $CD45^+$ TCRγδ cells (cluster IX, $\beta = 0.05$, $p = 0.03$). We also found a negative correlation between IL-17A and cluster VIII ($\beta = -0.28$, $p = 0.019$).

Combining all cervical immune variables (cytokines and immune cell populations) in a multiple factor analysis showed a trend for differential clustering of samples originating from HPV focal infections and from uninfected women (Fig. 2B). The axes indicate that HPV focal infections were negatively correlated with IFN-γ and IL-17a concentrations and frequency of CD16^{+} granulocytes (clusters I and II) (Fig. 2C). Conversely, the main vectors associated with HPV focal infection were CD45^{low} TCR$\gamma\delta$ cells (cluster VII), and cluster VIII (Fig. 2C).

Viral load kinetics

For all 126 participants with at least one HPV genotype detected, we estimated the virus load in all the cervical smears collected at each on-site visit for 13 HPV genotypes using a sensitive and specific quantitative Polymerase Chain Reaction (qPCR) protocol (*29*). The number of viral copies was normalised by that of a cellular gene (albumin). We could monitor 160 infections, including 28 complete infections (18%), 99 left-censored where participants were enrolled as positive (62%), and 69 right-censored where clearance was not observed (43%).

Given the longitudinal nature of our data, we turned to the field of viral kinetics (*30*) and developed Bayesian non-linear mixed-effects models (*31*, *32*). We described virus dynamics with five parameters capturing an increasing slope, a plateau, and a declining slope (Fig 4A and Methods). This shape was motivated by the important frequency of left- and right-censored follow-ups and the fast rate of reaching the plateau, which a simpler model with two slopes could not capture. Moreover, a similar plateau was observed to emerge in a previous mathematical model of HPV dynamics in squamous epithelia (*33*).

The resulting model parameter estimates captured the per-participant variability in normalised virus load values and exhibited wider uncertainty in censored follow-ups (Fig. 3). The population average of the mixed effect model (Fig. 4B) indicated that infections lasted 14 months (95% Credibility Interval, CrI, 11 to 18), with a 12 months (95% CrI: 10 to 15) plateau at 11

virus genomic copies per cell (95% CrI: 5 to 21). According to the model, 90% of the infections clear within three years, which is in line with earlier studies (*7*).

Immune kinetics

We then used the same method but with a different model to analyse the flow cytometry (FCM) time series. We transformed the cell population proportions using centered log-ratios (*34*) and assumed a two-slope model with matching dates of the beginning and end of the infection to the virus load fit (Fig. 4A). At the population level, we have identified distinct clusters of cells that exhibit similar kinetics during the course of infection (Fig. 4C). We have observed that a group of cells clusters, namely I and II, associated with the innate immune response, increased in relative proportion after the onset of infection. Another group of cell clusters, VII and VIII, exhibited a smaller and later peak during the course of infection. In contrast, a group of cells that are associated with the adaptive immune response, namely clusters VI, IX, X, and XI, decreased in frequency over the course of the infection. Moreover, we also noted a decline in the frequency of innate immune cells in clusters III, IV, and V during the infection. Remarkably, this clustering was also observed when examining inter-individual variation (Fig. S7).

We assumed the same two-slope model for the cytokines concentration dynamics in the cervix. At the population level, CCL20 increased over the course of the infection, and IFNγdecreased, while the other cytokines stayed steady (Fig. 4D), although with an important variability between participants. When looking at variation between participants, we found that the concentrations of CCL20 and CXCL10 were closely correlated, and negatively correlated to those of IL-17A and IFNγ (Fig. S8).

Finally, circulating IgG and IgM antibodies specifically targeting 10 HPV genotypes were quantified using a multiplex serology assay (*21*, *35*). We assumed a classical Bateman function for the dynamics (*36*) and only considered IgG and IgM specific to the infecting HPV genotype.

This limited the analysis to 55 infections in 37 individuals but still allowed us to identify a marked difference between IgG and IgM with a steeper decline of the latter (Fig. 4E). The individual data also showed that some infected women did not seroconvert after clearing the infection (4 out of 33, 12%).

Linking viral dynamics and immunity

We then compared the infection duration and the magnitude of the virus load with the immune response. For multiply infected individuals, we focused on the longest infection, which also generally had the highest plateau viral load (Fig. S6). The analysis was done using partial least square (PLS) regressions because of the compositional (and therefore highly correlated) nature of the data.

The regression explained a third of the variance in infection duration ($R^2_{adj.} = 0.33$), which was found to be significantly correlated with the mean concentration of IFNγ and the mean frequency of FCM clusters IX and VIII, but negatively associated with CXCL10 (Fig. 5A). Furthermore, HPV species α5 had a significantly shorter infection duration than the reference species α9 (which includes HPV16). The strong association between the multiply-infected status and the infection duration we identified was expected since we only kept the longest infection per participant in the model. Finally, for a smaller subset of participant infected by a genotype we could identify both with serology and qPCR, being seropositive in IgGs beforehand led to shorter infections (10 months, 95% CI: 5.6-17) than in seronegative individuals, even if they seroconverted (mean difference 1.8 months, 95% CI: 1.2 - 2.6) (Fig. 5C).

For the magnitude of the plateau virus load, the proportion of the variance explained by the PLS regression was lower ($R^2_{adj.} = 0.25$) but two immune variables, IFNγ mean concentration and cell cluster IX mean frequency, were positively associated with the plateau viral load (Fig. 5B). The HPV species had a strong impact on the plateau viral load and, compared to the reference

species α9, α6 had a higher viral load, whereas α5 had a lower one. The mean frequency of cluster VI was also negatively correlated with the plateau viral load. This cell population was most likely lymphocytes B, as underlined by the observation that among women with matching IgG data, cluster VI frequency was associated with the mean IgG titers in the serum during the infection (Fig. S9). Finally, women who were seropositive before the infection had a plateau viral load on average 7.6 times smaller (95% CI: 2.4-25) than those who seroconverted during the infection (Fig. 5D).

Discussion

While most HPV infections in young adults last less than two years (*4*, *6*, *7*, *15*), HPV clearance processes and mechanisms remain elusive. Thanks to the combination of dense monitoring, high-quality data, and powerful statistical models, we offer original insights into HPV-immunity clearance dynamics.

Given the little prior knowledge, we opted for a wide panel, studying both innate and adaptive immune responses. Focusing on lymphoid immunity and harnessing the power of unsupervised clustering enabled us to highlight the importance of TCRγδ cells on HPV dynamics, with at least three distinct subpopulations. Dominance of TCRγδ cells in mucosal immunity could explain their relative abundance in our analyses. This is consistent with recent studies that did not include these cells in their panels but found a relatively higher abundance of T cells in these tissues (*37*, *38*).

We also found a lower proportion of CD4 T cells (cluster X) in individuals with a focal HPV infection compared to uninfected individuals. Also, one population yet to be identified, cluster VIII, was increased in focal HPV infections. Based on its expression pattern, we hypothesise that it could contain ILCs or progenitors, although ILC3 are to be excluded given the lack of correlation between this cluster and IL-17A (Fig. 2) (*39*).

Among the infected participants for whom we could monitor viral kinetics by qPCR, Bayesian hierarchical modelling identified a positive correlation between the infection duration and only one of the three TCR$\gamma\delta$ populations (cluster IX with CD45$^+$ TCR$\gamma\delta$ cells). This highlights the diversity of these populations and suggests differential roles at specific times of the infection dynamic (*40*).

Our study also monitored the concentration of five cytokines in the cervix. Infection duration was positively correlated with IFNγ mean concentration, which is consistent with earlier results. Unexpectedly, longer infections were associated with decreased concentrations of CXCL10, although the release of this cytokine is usually stimulated by IFNγ (*41*). One interpretation is that averaging the overall response during the infection may overlook time-dependent patterns of the antiviral response. Another hypothesis could be that only the HPV infections that manage to evade the innate immune response can establish a more persistent infection, thereby triggering the adaptive immune response. In this case, CXCL10 would only be elevated during the early immune response. This is consistent with results from a comparable cohort indicating that persistence is associated with high levels of proinflammatory, Type-1, and regulatory cytokines (*25*).

Our viral load kinetics Bayesian model identified a weak correlation between infection duration and plateau viral load. Furthermore, our regression model suggested that the nature of the HPV genotype seems to exert a stronger influence on the plateau viral load than the host's immune response. However, the same model also points to a role of cluster VI (likely B lymphocytes) and prevalent IgG, which is in line with an impact of immune memory.

We did not observe any 'breakthrough' focal infection in the study and, as a consequence, vaccine status was not associated with infection duration or plateau viral load. We did, however, observe a trend towards shorter infections among vaccinated individuals, which could be attributed to a mild cross-protective mechanism. This is also consistent with our observation that

participants who were seropositive for an HPV genotype before being infected by this same genotype exhibited shorter infections with lower virus loads. This shows that natural immunity may provide protection against infection but is not sufficient to prevent it. Note also that the importance of the serological status imposes nuancing the role of the other factors on the duration of the infection and the plateau virus load.

Our work is limited to studying the path to chronic infections because participants were not followed after 24 months of infection by the same HPV (only 4 of the 126 infected women did not clear the infection in 18 months). Furthermore, although dense, our follow-up has a 4 months uncertainty window around 'singletons', i.e. HPV detection at a unique visit, and studies with denser follow-ups are required to better understand these infection events (*26*)

Our immunological analyses lay the ground for future work. Future extensions could be to investigate markers more related to myeloid immune cells. On the statistical side, adding a temporal dimension via the kinetics analyses allowed us to extract more information from the data by harnessing the longitudinal information inherent to the cohort. Future studies could build on existing within-host dynamics models (*33*) to estimate more biologically-relevant parameters, such as the 'burst size' of infected cells or the killing rate by the immune response.

Both the vaginal microbiota (*42*) and the immune response vary over the course of the menstrual cycle (*43*) with, for instance, fewer immunoglobulins during the luteal phase and, conversely, more IL-1α. Furthermore, the vaginal community state type has been associated with the risk of HPV detection (*26*). Investigating how menstrual cycles interact with the course of HPV infection dynamics would require a denser follow-up.

Cohort participants were followed for a mean duration of 290 days. Long-term follow-up of these women could yield valuable insights, especially thanks to new development in HPV full genome sequencing (*44*). For instance, it could help to estimate the prevalence of latent infections (*45*) but also further monitor the dynamics of chronic infections (*46*). Finally, it would

provide critical data on HPV within-host evolution, which could be associated with cancer development since HPV16 found in cervical cancers has a particular genomic signature with less variation in the E7 gene (*47*).

Beyond the case of HPVs, this system represents an opportunity to better understand the sometimes tenuous frontier between acute and chronic viral infections (*48*).

References

1. C. de Martel, M. Plummer, J. Vignat, S. Franceschi, *Int J Cancer* **141**, 664–670 (2017).
2. D. Forman *et al.*, *Vaccine* **30**, F12–F23 (2012).
3. R. L. Winer *et al.*, *N Engl J Med* **354**, 2645–54 (2006).
4. G. Y. Ho, R. Bierman, L. Beardsley, C. J. Chang, R. D. Burk, *N Engl J Med* **338**, 423–428 (1998).
5. A.-B. Moscicki *et al.*, *J Pediatr* **132**, 277–284 (1998).
6. R. P. Insinga, E. J. Dasbach, E. H. Elbasha, K.-L. Liaw, E. Barr, *Cancer Epidemiol Biomarkers Prev* **16**, 709–15 (2007).
7. A. V. Ramanakumar *et al.*, *BMJ Open* **6**, e011371 (2016).
8. M. Stanley, *Current Opinion in Virology* **51**, 106–110 (2021).
9. M. D. Ryser, E. R. Myers, R. Durrett, *PLoS Comput Biol* **11**, e1004113 (2015).
10. T. Beneteau, C. Selinger, M. T. Sofonea, S. Alizon, *PLoS Comput Biol* **17**, e1009352 (2021).
11. R. Herrero, P. González, L. E. Markowitz, *Lancet Oncol* **16**, e206–16 (2015).
12. J. Lei *et al.*, *New Engl J Med* **383**, 1340–1348 (2020).
13. L. Bruni *et al.*, *Lancet Glob Health* **4**, e453–63 (2016).
14. S. Alizon, C. L. Murall, I. G. Bravo, *Viruses* **9**, 293 (2017).
15. M. Schiffman, D. Solomon, *N Engl J Med* **369**, 2324–31 (2013).
16. C. P. Wild, Weiderpass, B. W. Stewart, Eds., *The World Cancer Report* (International Agency for Research on Cancer, Lyon, France, 2020).
17. J. G. Skeate, A. W. Woodham, M. H. Einstein, D. M. D. Silva, W. M. Kast, *Hum Vaccin Immunother* **12**, 1418–1429 (2016).
18. C. L. Murall, C. T. Bauch, T. Day, *Proc B* **282**, 20141069 (2015).
19. C. B. Woodman *et al.*, *The Lancet* **357**, 1831–1836 (June 2001).
20. C. L. Murall *et al.*, *BMJ Open* **9**, e025129 (2019).
21. C. L. Murall *et al.*, *Vaccine* **38**, 8167–8174 (2020).
22. M. Mollers *et al.*, *J Med Virol* **85**, 1379–1385 (2013).
23. J. A. Juno, G. Boily-Larouche, J. Lajoie, K. R. Fowke, *J Vis Exp* **89**, e51906 (2014).
24. L. M. Weber, M. Nowicka, C. Soneson, M. D. Robinson, *Commun Biol* **2**, 183 (2019).
25. M. E. Scott *et al.*, *International Journal of Cancer* **133**, 1187–1196 (2013).
26. R. M. Brotman *et al.*, *J Infect Dis* **210**, 1723–33 (2014).

27. C. Selinger *et al.*, *Immunol Res* **69**, 255–263 (2021).

28. L. J. P. Liebenberg *et al.*, *Nature Communications* **10**, 5227 (2019).

29. I. M. Micalessi, G. A. V. Boulet, J. J. Bogers, I. H. Benoy, C. E. Depuydt, *Clin Chem Lab Med* **50**, 655–61 (2012).

30. L. Canini, A. S. Perelson, *J Pharmacokinet Pharmacodyn* **41**, 431–443 (2014).

31. E. Comets, A. Lavenu, M. Lavielle, *J Stat Software* **80**, 1–41 (2017).

32. S. M. Kissler *et al.*, *New Engl J Med* **385**, 2489–2491 (2021).

33. C. L. Murall *et al.*, *PLoS Comput Biol* **15**, e1006646 (2019).

34. J. Aitchison, *Lecture Notes-Monograph Series* **24**, 73–81 (1994).

35. T. Waterboer *et al.*, *Clin Chem* **51**, 1845–1853 (2005).

36. E. R. Garrett, *J. Pharmacokinet. Biopharm.* **22**, 103–128 (1994).

37. B. Shannon *et al.*, *Mucosal Immunology* **10**, 1310–1319, ISSN: 1935-3456 (2017).

38. A. M. Zaki *et al.*, *Front. Microbiol.* **13** (June 2022).

39. M. D. Hazenberg, H. Spits, *Blood* **124**, 700–709 (2014).

40. D. Van hede *et al.*, *Proc Nat Acad Sci USA* **114** (2017).

41. A. D. Luster, J. C. Unkeless, J. V. Ravetch, *Nature* **315**, 672–676 (1985).

42. P. Gajer *et al.*, *Sci Transl Med* **4**, 132ra52 (2012).

43. S. M. Hughes *et al.*, *BMC Med* **20**, 353 (2022).

44. A. Holmes *et al.*, *Genomic Med* **1**, 1–16 (2016).

45. P. E. Gravitt, *J Clin Invest* **121**, 4593–4599 (2011).

46. C. E. Depuydt *et al.*, *Cancer Med* **4**, 1294–1302 (2015).

47. L. Mirabello *et al.*, *Cell* **170**, 1164–1174.e6 (2017).

48. H. W. Virgin, E. J. Wherry, R. Ahmed, *Cell* **138**, 30–50 (2009).

Acknowledgments

This project has received funding from the European Research Council (ERC) under the European Union's Horizon 2020 research and innovation programme (grant agreement No 648963, to SA).

The authors acknowledge further support from the Centre National de la Recherche Scientifique, the Institut de Recherche pour le Développement, the Fédération Hospitalière Universitaire InCH of Montpellier, the Fondation pour la Recherche Medicale (to TK), the Ligue contre le Cancer (to TB), and the Agence Nationale de la Recherche contre le Sida (ANRS-MIE, to NT and OS).

The authors acknowledge the ISO 9001 certified IRD i-Trop HPC (member of the South Green Platform) at IRD Montpellier for providing HPC resources that have contributed to the research results reported within this article (bioinfo.ird.fr and www.southgreen.fr).

The raw data and R scripts used will be deposited on the Zenodo server upon publication.

Supplementary materials

Materials and Methods

Supplementary Results

Figures S1 to S8

Tables S1 to S9

References (S1-S17)

Ethics, competing interests, and authors' contributions

Figures captions

Figure 1: **Unsupervised clustering of flow cytometry data from cervical smears.** A) Highlighting 11 homogeneous populations using UMAP clustering on data from samples without HPV or positive for a 'focal' HPV infection, B) Comparison of the clusters frequencies based on infection status, and C) Cluster annotation and fold change (FC) values shown in panels A and B. FC were calculated by an abundance analysis with diffcyt-DA-edgeR adjusted with a Benjamini-Hochberg test.

Figure 2: **Local immune response in HPV-infected and uninfected women.** A) Correlation matrix between the local density of five cytokines and the proportion of the 11 cell clusters from Figure 1. B) Sample clustering based on focal HPV infection status. C) Axes of a multiple factor analysis based on FCM and cervical cytokines and chemokines. In A, colors indicate the coefficient of pairwise regressions (only p-values lower than 10% are shown).

Figure 3: **Virus load kinetics for 160 HPV genital infections in 75 women.** Each panel corresponds to one participant and shows the number of HPV genome copies per number of human genome copies resulting from a three-slopes hierarchical Bayesian model. The lines show the posterior median trajectory and shaded area the 95% credibility interval. Open circles indicate values below the limit of detection. The letter before the anonymity number (above each panel) indicates whether the participant was vaccinated (V) or not (N).

Figure 4: **Population predictions of virus and immune kinetics in HPV infections.** A) Representation of the parameters governing the descriptive models. The viral kinetics model is governed by five parameters: plateau virus load ψ_d, time to the midpoint of the infection t_{mid}, growth phase duration ψ_a, plateau duration ψ_b, and clearance phase duration ψ_c. The FCM and cytokines kinetics models are governed by five parameters: time of infection t_{inf}, time of HPV clearance t_{clear}, basal value ψ_e, peak value ψ_f and peak time ψ_g. B) Population prediction of virus load dynamics. As in all the panels, the black thick line shows the median trajectory, the shaded area the 95% highest posterior distribution, each dot represents an observation, and thin lines show observed trajectories of individual infections. C) Population prediction for immune cell dynamics in HPV infections. Cell proportions are transformed with a centered log-ratio. D) Population prediction for cytokines dynamics in HPV infections. In panels C and D, time is normalized between 0 (infection) and 1 (clearance). E) Prediction of IgG (light green) and IgM (dark green) kinetics before and during HPV infections. MFI stands for mean fluorescence intensity.

Figure 5: **Factors associated with HPV infection duration and plateau viral load.** A) Outcome of partial least squares (PLS) regressions between the infection duration and the immune response summary statistics ($R^2_{adj} = 0.33$), and B) between the viral load during the plateau and the immune response summary statistics ($R^2_{adj} = 0.25$). Variables with a 95% CI different from 0 are shown in brighter colors (yellow for a positive correlation and purple for a negative one). The HPV reference species is α9, which includes HPV16. C) Association between the inferred timing of seropositivation on infection duration and D) plateau virus load. This timing has a significant effect on the infection duration ($F[2, 37] = 4.3$, $p = 0.023$) and on the plateau viral load ($F[2, 41] = 7.6$, $p = 1.5\ 10^{-3}$). Colors indicate vaccination status and shapes the genotype status (*i.e.* HPV16 or HPV18).

Figure 1

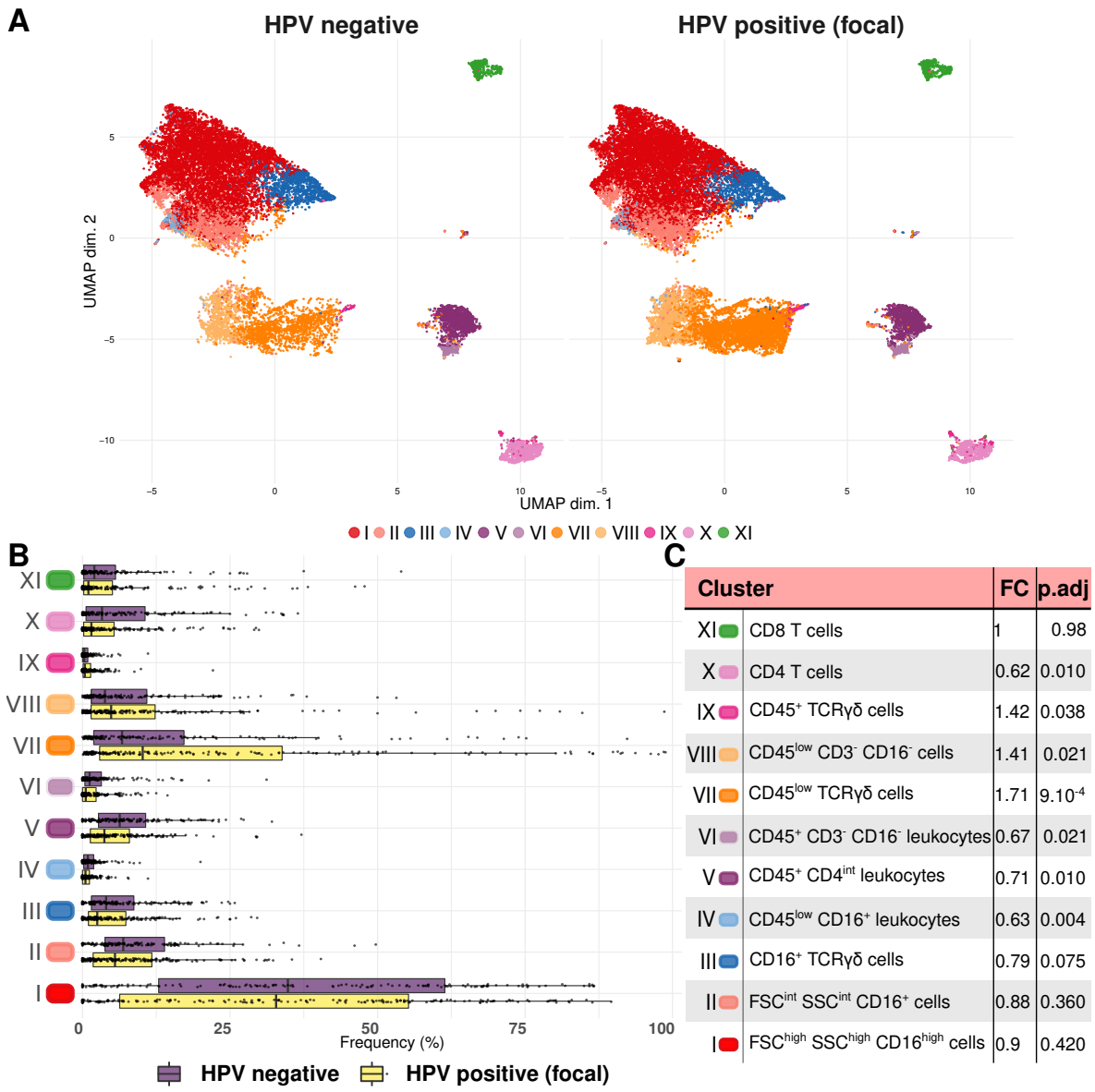

Cluster		FC	p.adj
XI	CD8 T cells	1	0.98
X	CD4 T cells	0.62	0.010
IX	CD45^{+} TCRγδ cells	1.42	0.038
VIII	CD45^{low} CD3^{-} CD16^{-} cells	1.41	0.021
VII	CD45^{low} TCRγδ cells	1.71	9.10^{-4}
VI	CD45^{+} CD3^{-} CD16^{-} leukocytes	0.67	0.021
V	CD45^{+} CD4^{int} leukocytes	0.71	0.010
IV	CD45^{low} CD16^{+} leukocytes	0.63	0.004
III	CD16^{+} TCRγδ cells	0.79	0.075
II	FSC^{int} SSC^{int} CD16^{+} cells	0.88	0.360
I	FSC^{high} SSC^{high} CD16^{high} cells	0.9	0.420

Figure 2

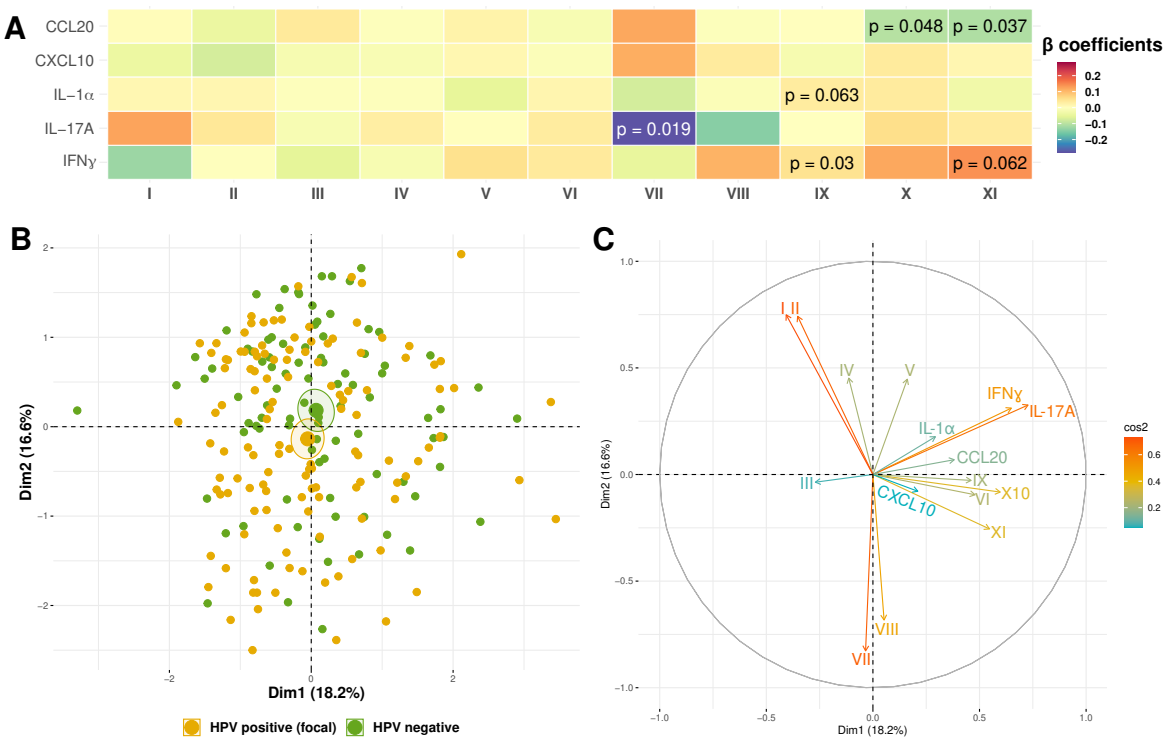
A
CCL20
CXCL10
IL−1α
IL−17A
IFNγ
p = 0.048
p = 0.037
p = 0.063
p = 0.019
p = 0.03
p = 0.062
I
II
III
IV
V
VI
VII
VIII
IX
X
XI
β coefficients
0.2
0.1
0.0
−0.1
−0.2
B
Dim2 (16.6%)
Dim1 (18.2%)
HPV positive (focal)
HPV negative
C
Dim2 (16.6%)
Dim1 (18.2%)
cos2
0.6
0.4
0.2
I II
IV
V
IFNγ
IL-17A
IL-1α
CCL20
IX
X10
VI
XI
III
CXCL10
VIII
VII

Figure 3

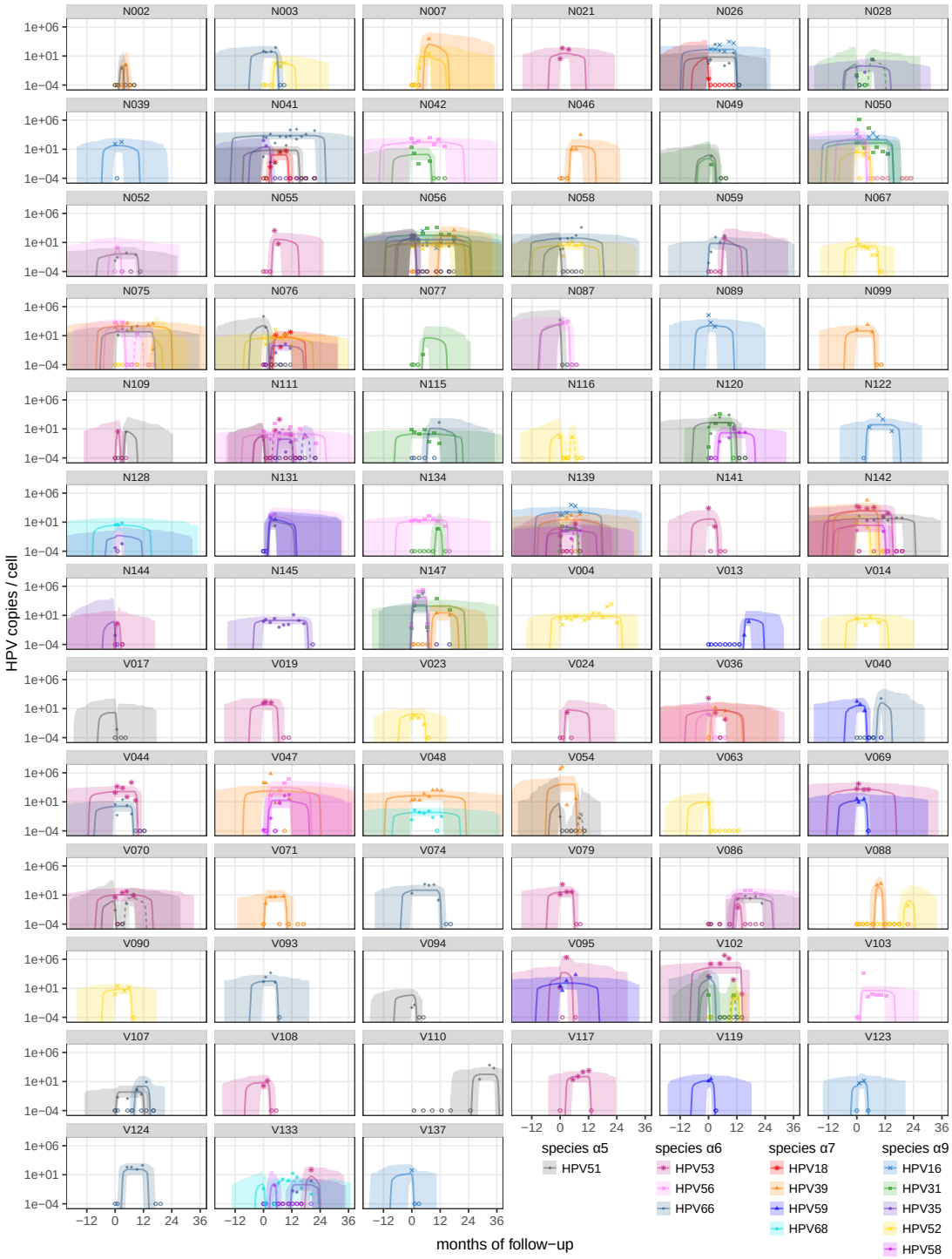
N002
N003
N007
N021
N026
N028
N039
N041
N042
N046
N049
N050
N052
N055
N056
N058
N059
N067
N075
N076
N077
N087
N089
N099
N109
N111
N115
N116
N120
N122
N128
N131
N134
N139
N141
N142
N144
N145
N147
V004
V013
V014
V017
V019
V023
V024
V036
V040
V044
V047
V048
V054
V063
V069
V070
V071
V074
V079
V086
V088
V090
V093
V094
V095
V102
V103
V107
V108
V110
V117
V119
V123
V124
V133
V137
1e+06
1e+01
1e−04
HPV copies / cell
−12
0
12
24
36
months of follow−up
species α5
HPV51
species α6
HPV53
HPV56
HPV66
species α7
HPV18
HPV39
HPV59
HPV68
species α9
HPV16
HPV31
HPV35
HPV52
HPV58

Figure 4

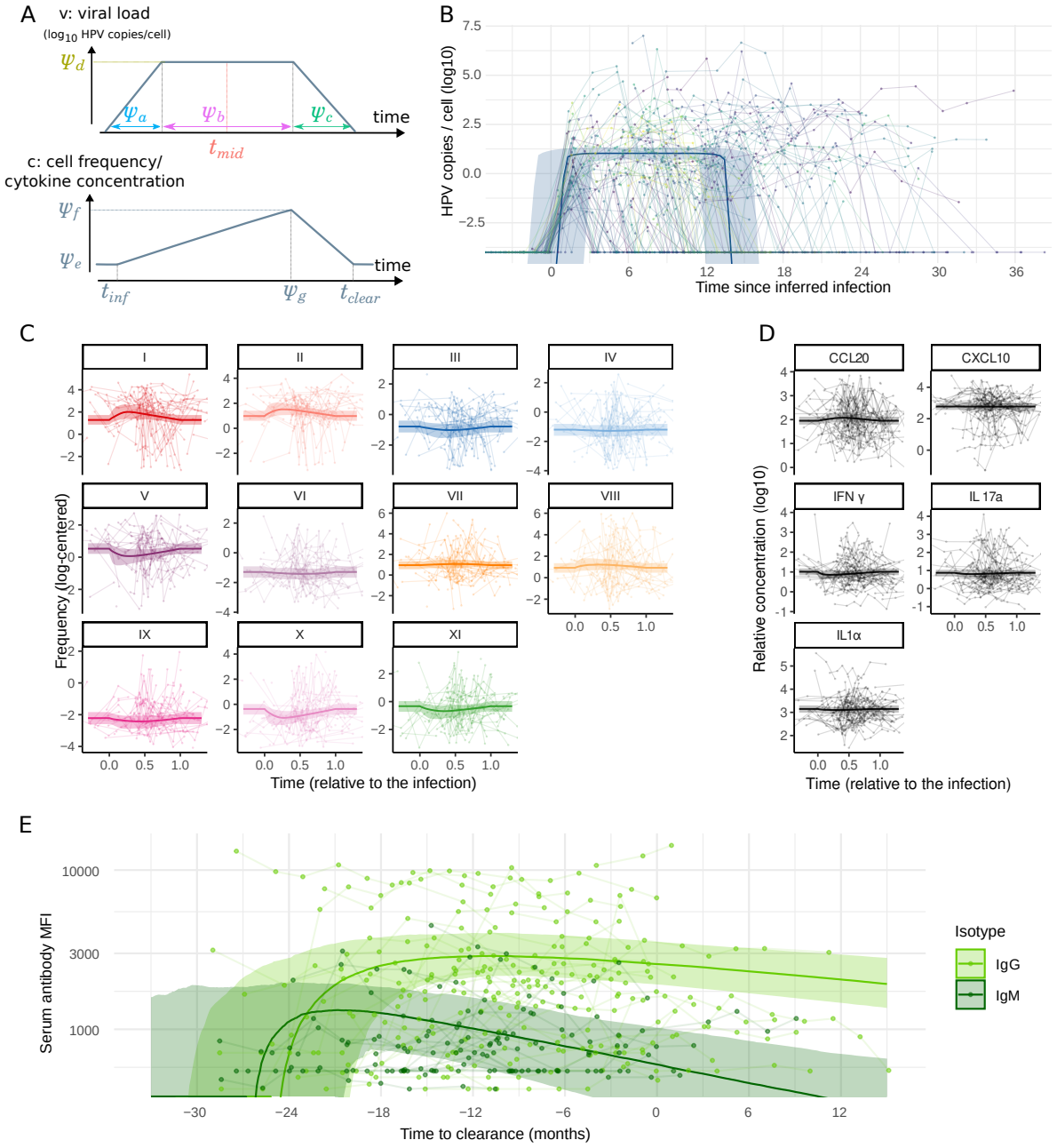
A
v: viral load
(log10 HPV copies/cell)
time
c: cell frequency/
cytokine concentration
time
B
HPV copies / cell (log10)
Time since inferred infection
C
Frequency (log-centered)
Time (relative to the infection)
D
Relative concentration (log10)
Time (relative to the infection)
E
Serum antibody MFI
Time to clearance (months)
Isotype
IgG
IgM

Figure 5

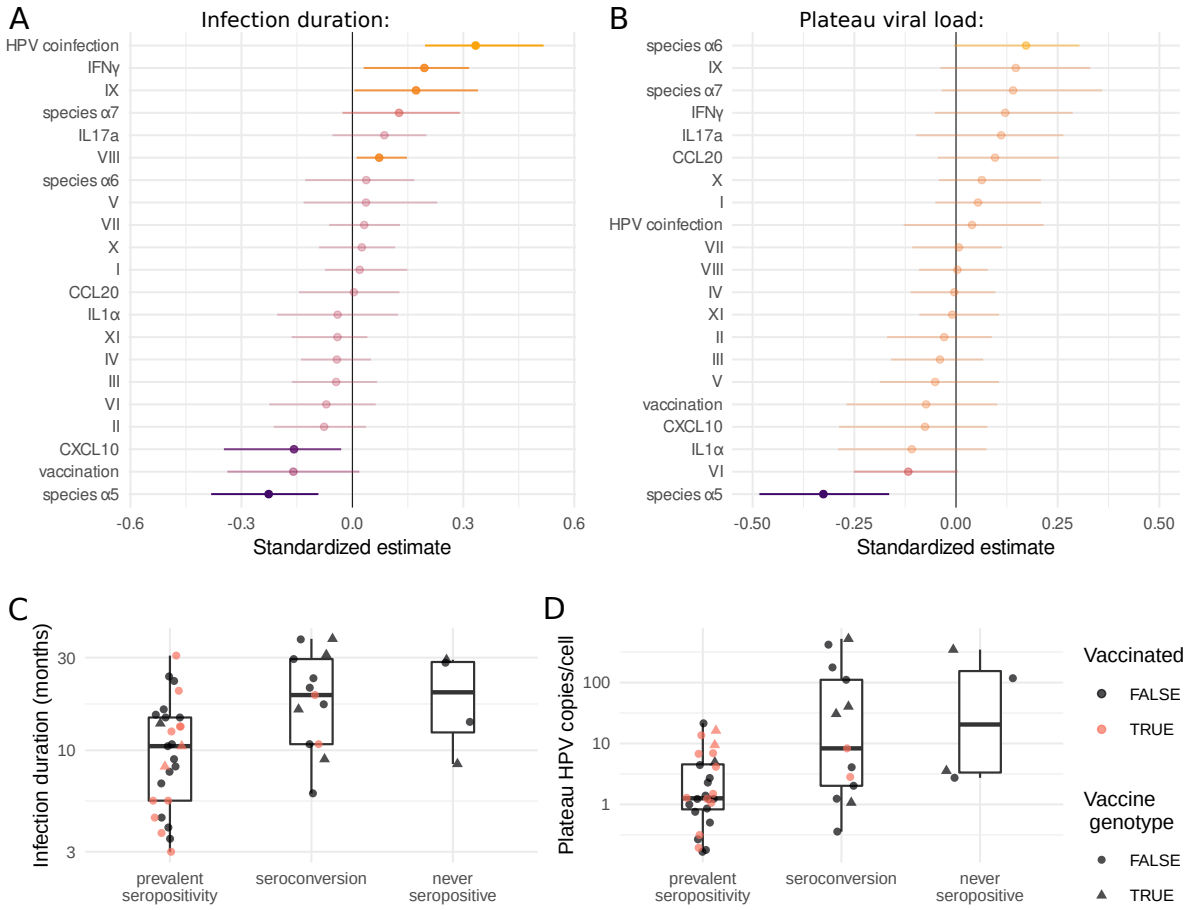
A
Infection duration:
HPV coinfection
IFNγ
IX
species α7
IL17a
VIII
species α6
V
VII
X
I
CCL20
IL1α
XI
IV
III
VI
II
CXCL10
vaccination
species α5
-0.6
-0.3
0.0
0.3
0.6
Standardized estimate
B
Plateau viral load:
species α6
IX
species α7
IFNγ
IL17a
CCL20
X
I
HPV coinfection
VII
VIII
IV
XI
II
III
V
vaccination
CXCL10
IL1α
VI
species α5
-0.50
-0.25
0.00
0.25
0.50
Standardized estimate
C
Infection duration (months)
30
10
3
prevalent seropositivity
seroconversion
never seropositive
D
Plateau HPV copies/cell
100
10
1
prevalent seropositivity
seroconversion
never seropositive
Vaccinated
FALSE
TRUE
Vaccine genotype
FALSE
TRUE